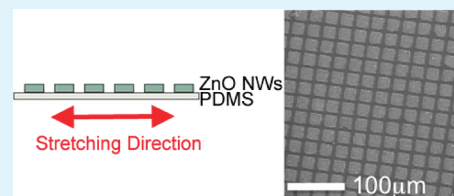


# Zinc Oxide Nanowire Rigid Platforms on Elastomeric Substrates

James S. Bendall,\* Ingrid Graz,<sup>†</sup> and Stéphanie P. Lacour<sup>‡</sup>

Nanoscience Centre, University of Cambridge, 11 JJ Thomson Ave, Cambridge, United Kingdom

**ABSTRACT:** Zinc oxide nanostructured thin films are transparent semiconducting ceramics increasingly used in a wide range of integrated devices. This paper outlines a simple strategy to integrate arrays of zinc oxide nanostructured thin films on elastomeric substrates using templated patterning. The arrays are robust to large uniaxial strains (up to 20% strain), do not fracture, and maintain electrical functionality. The integration of brittle nanostructured semiconducting materials on elastomeric substrates opens promising routes for the manufacture of deformable and stretchable electronics.



**KEYWORDS:** stretchable electronics, zinc oxide nanowires, silicone elastomer

Zinc oxide (ZnO) is an important technological material: with a large direct band gap (3.37 eV) it is transparent; it also exhibits piezo-electric properties ( $d_{33} = 10 \text{ pC/N}$ ).<sup>1</sup> It can be processed in bulk, thin-film or nanostructured forms, and is suitable for applications ranging from optoelectronics and solar cells to transparent electronics and electro-mechanical transducers. ZnO nanowire (NW) films, i.e., forest of wires (aligned or not) grown from a seed layer, are of particular interest for transducing applications such as solar cells and chemical sensors, where the surface area of the electrode or trapping material must be as large as possible.

Films of ZnO nanowires can be prepared with a variety of techniques such as chemical vapor deposition (CVD),<sup>2</sup> hydrothermal<sup>3</sup> or electrochemical<sup>4</sup> growths, and sol-gel deposition.<sup>5</sup> The carrier substrate is typically a conductive glass (fluorine doped tin oxide (FTO) or indium tin oxide (ITO) coated wafer) or a semiconductor wafer. The deposition of ZnO nanowires at low temperature, i.e.  $<100^\circ\text{C}$ , is a prerequisite for applications where the carrier substrate is a compliant polymer e.g., for flexible thin-film solar panels and conformable pressure sensing arrays. The hydrothermal method conducted at  $<90^\circ\text{C}$  in a noncorrosive chemical environment is a promising technique to form the nanostructure film directly on polymeric substrates.<sup>6</sup>

Elastomers such as silicones and polyurethanes are finding an unexpected field of application in stretchable electronics, i.e., a new class of large-area circuitry, which is designed to survive extreme and three-dimensional deformations. Rollable touch screens,<sup>7</sup> electronic eyes,<sup>8</sup> artificial skins,<sup>9,10</sup> stretchable RF electronics,<sup>11</sup> and ultracompliant bioelectronics interfaces<sup>12</sup> are some of the emerging applications for stretchable electronics. Elastomers are unconventional substrates for microelectronics. Today, research groups are actively exploring a range of micro-nanofabrication processes that will enable elastic circuitry.

In this paper, we demonstrate that ZnO NW films can be grown onto the elastomer and are suitable active materials for stretchable electronics. We report on the growth and morphology of ZnO NWs on PDMS. In conjunction with a stretchable thin gold film, we show that there is potential for stretchable ZnO-based devices to be easily synthesized on the ultracompliant

substrate. We further investigate the mechanical behavior of ZnO NW films on PDMS under tensile strain. We show that, by patterning the film into  $<20 \mu\text{m}$  side platforms, macroscopic strain of up to 20% can be reversibly applied to the elastomeric structure and does not induce mechanical failure in the ZnO NW platforms.

## MATERIALS AND METHODS

**ZnO NW Growth.** Zinc oxide nanowires are grown via a low-temperature hydrothermal route, using a two-step method of seed deposition and nanowire growth.<sup>13</sup> The process flow is presented in Figure 1a. The substrate is a 1 mm thick membrane of polydimethylsiloxane PDMS (Dow Corning Sylgard 184, 10:1 w-w); no surface treatment is used. A Zn seed layer of 100 nm thickness is deposited onto the surface of the substrate using an Emitech sputter coater fitted with a high purity zinc target (Goodfellow 99.95+% purity), operated at 100 mA and  $1 \times 10^{-3} \text{ mbar}$ . Patterned seed layers are prepared by shadow masking using copper TEM grids; the rest of the PDMS surface is protected by a polyimide foil so that the NWs only grow within the TEM grid. Crucially no annealing is required prior to ZnO growth. Many alternative seed layer preparations involve the thermal decomposition and oxidation of a sprayed zinc salt solution to produce nanocrystals (i.e., nucleation sites) of ZnO which typically take place at temperatures above  $400^\circ\text{C}$ , making them incompatible processes with most plastic and elastomeric substrates. The seeded substrate is then placed into a growth solution containing 0.05 M zinc nitrate and 0.05 M hexamethylenetetramine (HMT) held at  $92^\circ\text{C}$  and undergoes in situ oxidation.<sup>14</sup> After a 2 h growth time, the substrate is removed from the solution, rinsed with deionized water and dried under a stream of nitrogen gas.

**Morphological Characterization.** The ZnO NWs on PDMS are imaged with a Leo 1530VP scanning electron microscope (SEM), operated at 7 keV. The hydrothermal growth method produces nanowires, with diameters of  $\sim 30 \text{ nm}$  and lengths of  $900 \text{ nm} \pm 100 \text{ nm}$  when grown on standard “hard” substrates (such as FTO-coated glass). The

**Received:** May 24, 2011

**Accepted:** July 8, 2011

**Published:** July 09, 2011

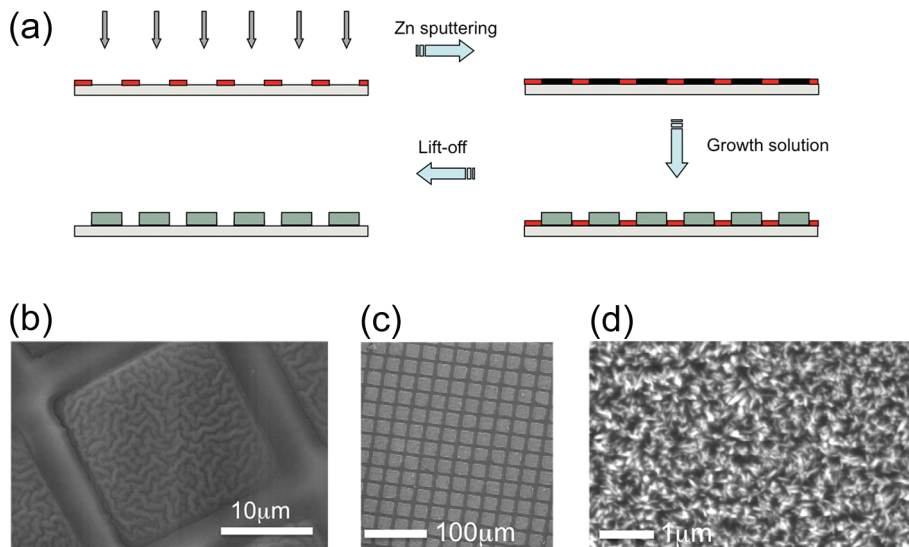


**Figure 1.** (a) Process flow for the preparation of patterned NW growth on elastomeric substrates. Light gray represents the PDMS substrate, red is the shadow mask, black represents the Zn seed layer, dark gray represents the NWs. SEM images of (b) the patterned Zn seed layer and (c) the patterned ZnO NW film on PDMS. (d) Zoom on the patterned ZnO NWs.

nanowires are vertically aligned with their *c*-axis nearly perpendicular to the substrate plane, and are highly crystalline structures with good uniformity across the device's entire active area.<sup>15</sup>

**Uniaxial Stretching.** The 3.5 mm diameter TEM grid is positioned at the center of the top surface of the PDMS membrane so that the applied strain is uniformly distributed across the NW matrix; no edge or clamping effects affect the observations. *In situ* stretching to 20% strain and imaging of the samples are conducted in a FEI Philips XL30 FEG ESEM equipped with a built-in tensiometer. Uniaxial stretching is also carried out in a home-built, LabView controlled, stretching apparatus coupled with a digital microscope (Keyence Ltd.). The PDMS membranes of ~40 mm length and 10 mm width are mounted between two clamps moving apart with micrometre precision. The stretching direction is parallel to the length of the PDMS strip, along the *x* direction. The samples are stretched and released in a 0% to 20% applied strain stretch cycle (calculated by  $\varepsilon_{\text{appl}} = \Delta L/L_0$  from the measured elongation of the strip  $\Delta L$  and its initial length  $L_0$ ) in steps of 1% strain within 60 s. Platform dimensions and interplatform distances are measured with an accuracy of about 3% along the *x* and *y* directions from optical micrographs taken during the stretching cycles, and averaged over a  $3 \times 3$  platform array.

**ZnO NW Diodes on PDMS.** Instead of growing the NWs on "bare" PDMS, they are prepared on a thin film of chromium/gold/chromium (5/50/5 nm) preliminary deposited on the PDMS substrate and used as a bottom contact. The gold electrode is patterned as a dog bone shaped stripe of 1 mm width, 5 mm length and with  $4 \text{ mm} \times 4 \text{ mm}$  contact pads. The Zn seed film is subsequently sputtered through a TEM grid, which is mounted in the middle of the Au stripe, and placed in the ZnO growth solution. After growth, the substrate is washed in deionized water and dried under a stream of nitrogen gas and the TEM grid carefully removed. A conformal 600 nm thick coating of insulating parylene C is then deposited using a Labcoater 2010 (SCS Coatings) over the complete substrate area, and etched back with oxygen plasma (Plasma Lab System 100 (ICP180), Oxford Instruments) to expose the tips of the NWs. The top electrode prepared on a second PDMS membrane coated with a Cr/Au bilayer completes the device. The parylene film ensures there is no short-circuit between the bottom and top gold electrodes. Device electrical testing is carried out using a Keithley 4200 Semiconductor Characterization system.

## RESULTS

**Growth of ZnO NW Devices on Elastomeric Substrates.** Thin films of ZnO NWs grown on plain (nonpatterned) Zn seed layers are covered with random macroscopic cracks, which are found to systematically appear when the growth surface area is larger than  $250 \mu\text{m} \times 250 \mu\text{m}$ . By patterning the Zn seed layer into platforms smaller than  $250 \mu\text{m} \times 250 \mu\text{m}$ , crack-free ZnO NW films can be produced.

Two patterns are studied based on TEM grid masks of 1000 mesh (20  $\mu\text{m}$  side, 6  $\mu\text{m}$  spacing) and 100 mesh (200  $\mu\text{m}$  side, 50  $\mu\text{m}$  spacing). In both mesh sizes, platforms cover about 80% of the grid surface area.

The 100 nm thick Zn seed layer sputtered on PDMS through the TEM grid spontaneously wrinkles; the buckles' wavelength is approximately 1  $\mu\text{m}$  as shown in Figure 1b. Buckling is a well-known mechanism for stress relief in stiff thin films deposited on compliant substrate.<sup>16,17</sup> Images of the 1000 mesh films (Figure 1c) indicate that as-prepared NW platforms are crack-free and uniform in size and shape; no nanowires grow on the bare (non-Zn-coated) PDMS. Zooming-in on the individual platforms reveals vast arrays of NWs as illustrated Figure 1d. The shape and dimensions of the nanowires are identical to those grown on hard substrates, with diameters of  $3 \text{ nm} \pm 5 \text{ nm}$  and lengths of  $1 \mu\text{m} \pm 50 \text{ nm}$ .

**ZnO NW Diodes on PDMS Substrate.** Schottky diodes on PDMS are fabricated to assess the electrical properties of the ZnO nanowires on a soft substrate. Panels a and b of Figure 2 present a schematic and top view picture of the NW devices on PDMS. The overlapping top electrode (Au on PDMS) is 200  $\mu\text{m}$  wide and 1000  $\mu\text{m}$  long, and thus covers about 320 NW platforms of 20  $\mu\text{m}$  side; the bottom and top electrodes run perpendicularly. The measured current–voltage  $I(V)$  therefore corresponds to the electrical response of a dense network of ZnO nanowires. It is not clear why the observed macroscopic cracks and wrinkles form in the parylene overlay (inset of Figure 2b); they may be initiated during the ICP dry etch step where local heating may expand (then contract) the elastomeric substrate.

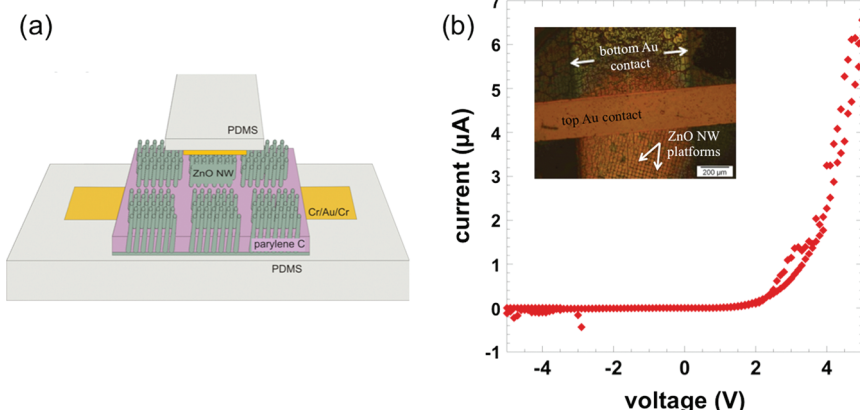


**Figure 2.** (a) Architectural schematic of ZnO NW device constructed using parylene deposition and subsequent ICP-etch. (b) Typical  $I(V)$  curve measured through an array of 20  $\mu\text{m}$ -side ZnO NW platforms on PDMS; the voltage is swept from  $-5$  V to  $5$  V and back to  $-5$  V. Inset: top view of the ZnO NW device embedded in PDMS; the 1  $\mu\text{m}$  long ZnO NWs are coated with parylene and sandwiched between two Au film-on-PDMS electrodes. The NW density is about  $1 \times 10^5/20 \times 20 \mu\text{m}^2$  platform.

The  $I(V)$  characteristic of the ZnO NW Schottky devices are recorded at room temperature and swept from  $-5$  V to  $5$  V back to  $-5$  V; the PDMS substrate is not stretched. The  $I(V)$  plot shown Figure 2b illustrates the typical rectifying behavior of the macroscopic device in the negative voltage regime. The turn-on voltage is approximately 3 V; no hysteresis is observed. It was not possible to record reliable electrical data when the PDMS substrate was held stretched under tensile strain. Further process optimization is required to deposit the parylene film only over the ZnO NW platforms rather than across the whole of the NW platform network.

**Stretching Behavior of ZnO NW Patterned Arrays.** Four types of Zn-based films on PDMS are evaluated under uniaxial stretching: (i) Zn seed layer, (ii) unpatterned ZnO NW film, (iii) patterned Zn seed layer and (iv) patterned ZnO NW films.

Unpatterned Zn seed layers on PDMS are very brittle: large and uncontrollable cracks propagate across the 100 nm thick film and are often visible immediately after fabrication. Such samples were not stretched to 20% strain.

When the Zn seed layer is patterned into small platforms defined by the TEM grid (100 and 1000 mesh), the Zn film appears more robust to mechanical loading. After fabrication, the Zn film is randomly wrinkled (Figure 1b). Upon stretching, wrinkles in the direction of the applied elongation form in the Zn film. At 10% strain, no associated cracking can be seen. At 20% strain, large cracks perpendicular to the stretching direction appear together with pronounced wrinkling in the Zn platforms (in direction of the applied strain). The wrinkles parallel to the applied strain result from the associated Poisson compression (PDMS Poisson ratio  $\nu_{\text{PDMS}}$  is 0.5). This behavior is typical of hard coatings on soft substrates.<sup>18–20</sup>

ZnO NW films grown on an “unpatterned” Zn seed layer on PDMS are prone to uncontrollable fracture and wrinkling, delamination and distortion, similar to that seen for Zn thin films. Though in this configuration the Zn seed layer is in all likelihood already cracked before entering the growth solution, the brittleness of the ZnO layer on PDMS is further emphasized by the ceramic nature of the film, the large coefficient of thermal expansion (CTE) and swellability of PDMS (the substrate expands by about 2% in volume when placed in the 90 °C growth bath). Furthermore, when stretched, these cracks and

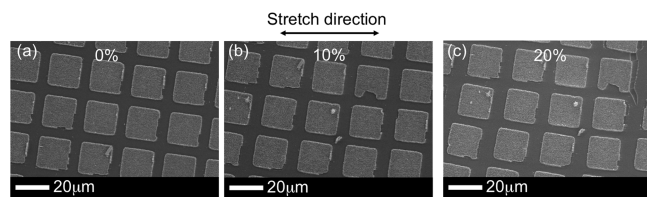


**Figure 3.** Imaging of patterned film of nanostructured ZnO on PDMS under increasing strain (a) 0, (b) 10, and (c) 20% at the same SEM magnification and on the same sample area. The stretching direction is in the  $x$ -direction with respect to the imaging. Because of slight misalignment of the grid with the stretching direction, there is a platform offset of 2° in the  $x$ -direction.

wrinkles are, unsurprisingly, seen to increase in size and frequency and the continuous films show a classic behavior observed for many brittle films on PDMS.<sup>20,21</sup> The cracks enlarge and open up perpendicular to the stretching direction while lateral buckling occurs simultaneously because of Poisson compression of the ceramic/elastomer.

When grown through a mesh template and seed layer, ZnO NW films on PDMS can withstand large mechanical stretching without cracking. We have investigated two mesh sizes (with 20 and 200  $\mu\text{m}$  side platform) and a single surface-area coverage ( $\sim 80\%$  of the substrate—within the TEM disk—is covered by the ZnO NWs).

In a 1000 mesh ZnO NW array, no cracks are observed under the SEM within the platforms even at 20% applied strain (Figure 3); the platforms remain intact. Surprisingly, the underlying PDMS seems to tear (Figure 3c). This was observed in most of the samples. The ZnO NW growth solution is an amine-based reagent, which tends to dissolve PDMS over prolonged or high concentration exposure.<sup>22</sup> The 2 h long ZnO NW growth may alter rather than dissolve the upper layer of the PDMS, leading to a more brittle material than bulk PDMS.

Figure 3 illustrates the elasticity of the ZnO NW matrix during a 20% stretch cycle. The platforms remain square and crack-free; the substrate elongation within the platforms is clearly visible with increasing strain.

The behavior of the 1000-mesh platforms can be described with the simple model published in.<sup>16</sup> Applied strain,  $\varepsilon_{\text{appl}}$ , is

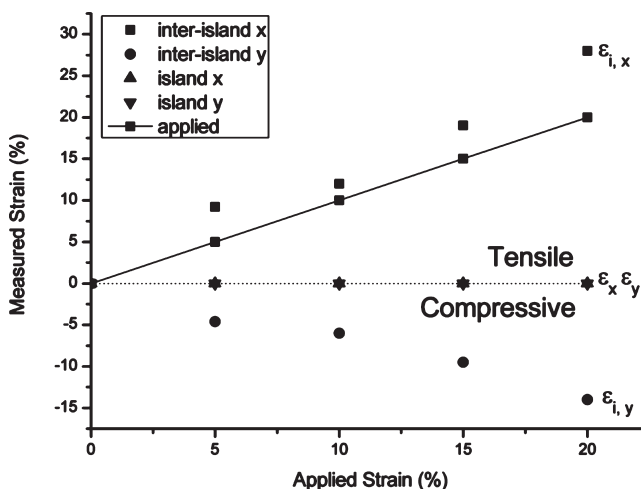


**Figure 4.** Measured strains in ZnO platforms and interplatform as a function of the applied strain for 1000 mesh platforms. Each value was determined from the platform dimensions and interplatform distances during applied strain. Dimensions were measured with an accuracy of 3% along the  $x$  and  $y$  directions from optical micrographs taken during the stretching cycles, and averaged over a  $3 \times 3$  platform array.

defined as

$$\varepsilon_{appl} = \frac{\Delta b}{a + b}$$

where  $a$  is the length of the side of the platform and  $b$  is the interplatform spacing distance, and assumes that  $a$  stays constant over stretching i.e. the platform does not deform. This is a valid assumption for this study since accurate measurements from the SEM micrographs show that the platform dimensions do not change during mechanical loading. The interplatform strains are calculated from the following formulas<sup>16</sup>

$$\varepsilon_{inter,x} = \left(1 + \frac{a}{b}\right) \varepsilon_{appl} \text{ and } \varepsilon_{inter,y} = -\nu_{sub} \left(1 + \frac{a}{b}\right) \varepsilon_{appl}$$

where  $\nu_{sub}$  is the Poisson ratio of the substrate, which is about 0.5 for PDMS.

The strains within the platforms and in-between the platforms, both in the  $x$  and  $y$  directions are calculated from the SEM pictures. Figure 4 shows a plot of the applied strain vs the respectively measured interplatform and platform strains in  $x$  and  $y$  directions for platforms of  $20 \mu\text{m}$  side. No visible change in the platform dimensions is measured (strain = 0%). Interplatform strain  $\varepsilon_{i,x}$  increases in the  $x$  direction ( $\varepsilon_{i,x} = 19\%$  at 15% applied strain) and  $\varepsilon_{i,y}$  decreases in the  $y$  direction ( $\varepsilon_{i,y} = 9.5\%$  at 15% applied strain). This behavior is indicative of an array of pads, which remains stiff and “undeformable”; the applied strain distributes throughout the surrounding PDMS. This was already observed in diamond-like carbon (DLC) platforms on PDMS; note however that the DLC film was much thinner (185 nm) and stronger than the ZnO (modulus >500 GPa).<sup>16</sup> We observe very large interplatform strains upon increase applied strain, reaching a maximum tensile strain of 30% in the  $x$ -direction and 15% compressive strain in the  $y$ -direction with an applied strain of 20%. Crucially, no change in platform size and no breakage are observed over the whole stretching cycle (i.e., stretching up to 20% and releasing back to 0%). No distortion is visible after unloading, indicating an almost fully elastic system. This inherent

ability to stretch to higher regimes, yet still retain their integrity, makes them ideal candidates for stretchable nanodevices.

Larger platform (100 mesh ZnO NW) arrays can be stretched but only to modest applied strain (<2%). Even under moderate applied strains of 4%, the platforms laterally distort, crack and buckle in a similar way to the continuous film. The failure of larger platforms shows that for the evaluated platform sizes (20 and  $200 \mu\text{m}$ ) and density (80% surface coverage), the integrity of the NW platforms to large applied stretch cycles can only be ensured for the smallest platforms. For 900 nm tall ZnO NW platforms on 1 mm thick PDMS, patterns must be no larger than  $20 \mu\text{m}$  side and  $6 \mu\text{m}$  apart in order to be protected from irreversible crack propagation.

## CONCLUSION

Our results demonstrate a suitable fabrication process for nanostructured zinc oxide platforms on elastomeric substrates. By adjusting the footprint and density of the NW platforms on PDMS, stretchable matrices can be produced where the brittle nanowire platforms remain crack free upon large mechanical deformation. The hydrothermal technique combining mild chemical growth environment and  $<100^\circ\text{C}$  process temperature can be used for a wide range of advanced nanomaterials such as hierachal structures and core–shell structures. Therefore these results provide the groundwork for nanowire-based integrated electrical devices on stretchable substrates. The ability to pattern electroactive NW arrays, which can sustain large deformations and retain their functionality makes the presented work is a promising approach for highly conformable electronic devices such as stretchable OLEDs or solar cells.

## AUTHOR INFORMATION

### Corresponding Author

\*E-mail: jsb53@cam.ac.uk.

### Present Addresses

<sup>†</sup>Currently at Soft Matter Physics, Johannes Kepler University, Linz, Austria.

<sup>‡</sup>Currently at Laboratory for Soft Bioelectronic Interfaces, EPFL, Lausanne, Switzerland.

## ACKNOWLEDGMENT

This research was part-funded by the European Community’s Seventh Framework Program (FP7/2007-2013) under Grant 227057, Project “INNOVASOL”, and the Royal Society. S.P.L. thanks Dr. Natalie Plank for preliminary discussions.

## REFERENCES

- (1) Xu, B.; Eric Cross, L.; Bernstein, J. J. *Thin Solid Films* **2000**, 377–378, 712–718.
- (2) Hong, W.-K.; Jo, G.; Sohn, J. I.; Park, W.; Choe, M.; Wang, G.; Kahng, Y H.; Welland, M. E.; Lee, T *ACS Nano* **2010**, 4, 811–818.
- (3) Vayssières, L. *Adv. Mater.* **2003**, 15, 464–466.
- (4) Elias, J.; Levy-Clement, C.; Bechelany, M.; Michler, J.; Wang, G. Y.; Wang, Z.; Philippe, L. *Adv. Mater.* **2010**, 22, 1607–1612.
- (5) Saifullah, M. S. M.; Subramanian, K. R. V.; Kang, D. J.; Anderson, D.; Huck, W. T. S.; Jones, G. A. C.; Welland, M. E. *Adv. Mater.* **2005**, 17, 1757–1761.
- (6) Plank, N. O. V.; Snaith, H. J.; Ducati, C.; Bendall, J. S.; Schmidt-Mende, L.; Welland, M. E. *Nanotechnology* **2008**, 19, 465603.

(7) Bae, S.; Kim, H.; Lee, Y.; Xu, X.; Park, J. -S.; Zheng, Y.; Balakrishnan, J.; Lei, T.; Ri Kim, H.; Song, Y. I.; Kim, Y. -J.; Kim, K. S.; Ozylmaz, B.; Ahn, J. -H.; Hong, B. H.; Iijima, S. *Nat. Nanotechnol.* **2010**, *5*, 574–578.

(8) Jung, I.; Xiao, J.; Malyarchuk, V.; Lu, C.; Li, M.; Liu, Z.; Yoon, J.; Huang, Y.; Rogers, J. A. *Proc. Natl. Acad. Sci. U.S.A.* **2011**, *108*, 1788–1793.

(9) Someya, T.; Kato, Y.; Sekitani, T.; Iba, S.; Noguchi, Y.; Murase, Y.; Kawaguchi, H.; Sakurai, T. *Proc. Natl. Acad. Sci. U.S.A.* **2005**, *102*, 12321–12325.

(10) Takei, K.; Takahashi, T.; Ho, J. C.; Ko, H.; Gillies, A. G.; Leu, P. W.; Fearing, R. S.; Javey, A. *Nat. Mater.* **2010**, *9*, 821–826.

(11) Cheng, S.; Wu, Z. *Lab Chip* **2010**, *10*, 3227–3234.

(12) Kim, D. -H.; Viventi, J.; Amsden, J. J.; Xiao, J.; Vigeland, L.; Kim, Y. -S.; Blanco, J. A.; Panilaitis, B.; Frechette, E. S.; Contreras, D.; Kaplan, D. L.; Omenetto, F. G.; Huang, Y.; Hwang, K. -C.; Zakin, M. R.; Litt, B.; Rogers, J. A. *Nat. Mater.* **2010**, *9*, 511–517.

(13) Bendall, J. S.; Visimberga, G.; Szachowicz, M.; Plank, N. O. V.; Romanov, S.; Sotomayor-Torres, C. M.; Welland, M. E. *J. Mater. Chem.* **2008**, *18*, 5259–5266.

(14) Plank, N. O. V.; Welland, M. E.; MacManus-Driscoll, J. L.; Schmidt-Mende, L. *Thin Solid Films* **2008**, *516*, 7218–7222.

(15) Plank, N. O. V.; Howard, I.; Rao, A.; Wilson, M. W. B.; Ducati, C.; Mane, R. S.; Bendall, J. S.; Louca, R. R. M.; Greenham, N. C.; Miura, H.; Friend, R. H.; Snaith, H. J.; Welland, M. E. *J. Phys. Chem. C* **2009**, *113*, 18515–18522.

(16) Lacour, S. P.; Wagner, S.; Narayan, R. J.; Li, T.; Suo, Z. *J. Appl. Phys.* **2006**, *100*, 014913.

(17) Bowden, N.; Brittain, S.; Evans, A. G.; Hutchinson, J. W.; Whitesides, G. M. *Nature* **1998**, *393*, 146–149.

(18) Genzer, J.; Groenewold, J. *Soft Matter* **2006**, *2*, 310–323.

(19) Lu, N.; Wang, X.; Suo, Z.; Vlassak, J. *J. Mater. Res.* **2009**, *24*, 379–385.

(20) Görre, P.; Wagner, S. *J. Appl. Phys.* **2010**, *108*, 093522.

(21) Experimental observations by the authors from a variety of thin film deposited on PDMS such as silicon oxide, silicon nitride, diamond like carbon, gold, copper, pentacene, amorphous silicon; unpublished data.

(22) Lee, J. N.; Park, C.; Whitesides, G. M. *Anal. Chem.* **2003**, *75*, 6544–6554.